State interactions and illumination of hidden states through perturbations and observations of new states: High energy resonance enhanced multiphoton ionization of HI

Helgi Rafn Hróðmarsson, Huasheng Wang, and Ágúst Kvaran

Citation: The Journal of Chemical Physics **142**, 244312 (2015); doi: 10.1063/1.4922892
View online: http://dx.doi.org/10.1063/1.4922892
View Table of Contents: http://scitation.aip.org/content/aip/journal/jcp/142/24?ver=pdfcov
Published by the AIP Publishing

State interactions and illumination of hidden states through perturbations and observations of new states: High energy resonance enhanced multiphoton ionization of HI

Helgi Rafn Hróðmarsson, Huasheng Wang, and Ágúst Kvaran[a)]
Science Institute, University of Iceland, Dunhagi 3, 107 Reykjavík, Iceland

(Received 24 March 2015; accepted 12 June 2015; published online 30 June 2015)

Hydrogen iodide, a Hund's case (c) molecule, serves as a benchmark compound for studying rich molecular state interactions between Rydberg and valence states as well as between Rydberg states at high energies (72 300–74 600 cm^{-1}) by mass resolved resonance enhanced multiphoton ionization (REMPI). Perturbations in the spectra appearing as deformations in line-positions, line-intensities, and linewidths are found to be either due to near-degenerate or non-degenerate interactions, both homogeneous and heterogeneous in nature. Perturbation analyses allow indirect observation as well as characterization of "hidden states" to some extent. Furthermore, new observable spectral features are assigned and characterized. © *2015 AIP Publishing LLC.* [http://dx.doi.org/10.1063/1.4922892]

I. INTRODUCTION

The electronic spectra of the hydrogen halides are of particular interest within the spectroscopic community due to the clarity and resolution of their spectral structures as well as the state interactions embedded within as perturbation effects. The spectra provide clear examples of interactions between Rydberg and valence states of varying strength and nature. They provide information about various photofragmentation and photoionization pathways which are of interest to a variety of other related fields such as atmospheric chemistry,[1,2] astrochemistry,[3,4] and photochemical syntheses.[5]

In addition to standard absorption spectroscopic studies of the hydrogen halides,[6–15] resonance enhanced multiphoton ionization (REMPI) analyses have been widely used, allowing states, which are regularly inaccessible by single photon selection rules to be formed. Most REMPI experiments have been conducted on HCl,[16–33] whereas a handful of studies of HBr[26,27,33–39] and HI[40–45] have been performed. Furthermore, some REMPI coupled velocity map imaging (VMI) studies have been performed on the hydrogen halides, highlighting various photoionization and photofragmentation pathways.[46–52]

The large atomic mass of iodine makes HI particularly interesting amongst the hydrogen halides due to its strong spin-orbit interactions. For the lighter hydrogen halides, such as HF and HCl, the spin and electronic orbital motions are coupled strongly to the molecular axis to give well defined projections on the internuclear axis, which along with the angular momentum of the nuclear motion (**R**) give the total angular momentum, **J** according the to Hund's case (a) classification. For HI, on the other hand, the coupling between **L** and **S** is stronger than the interaction with the internuclear axis, which makes only Ω well defined, resulting in the Hund's case (c) classification.[53] Nevertheless, it has become a custom in the literature to use analogous and comparable state assignments, more appropriate for Hund's cases (a) and (b), for all the hydrogen halides.[6–15]

The rotational spectroscopy of HI was first studied in the pioneering work by Price.[54] Later absorption experiments constructed a coherent database of excited Rydberg and ion-pair states of HI[13–15] as well as DI[14,15,55] and addressed several observed perturbations seen in the spectra. The first REMPI spectra of HI were published in 1994–1995.[40,41] These studies included new observations of spectral structures, but with some tentative assignments. These have recently been revisited with an emphasis placed on new observations as well as state interactions between Rydberg and valence (ion-pair and repulsive) states.[44,45] Among recent findings, the utilization of perturbation effects was used to illuminate interactions between an ion-pair state and a state that was "hidden" from REMPI detection.[45] The "hidden" state could either be a non-observable state due to selection rules or a state experiencing weak transition probabilities, which could possibly be detectable by other means, such as in standard absorption.

We will now present REMPI data of HI for the high energy two-photon excitation region of 72 300–74 600 cm^{-1} and analyses relevant to state interactions between Rydberg and valence states as well as between Rydberg states. Furthermore, new observations both for observable and "hidden" states are presented.

II. EXPERIMENTAL

The experimental apparatus as well as relevant equipment parameters are similar to that described in previous publications.[39,44,45] Therefore, only a brief experimental discussion will be given here.

Mass resolved REMPI data for a HI molecular beam were recorded. The beam was created by a jet expansion of a pure gas sample through a pulsed nozzle and ions

a)Author to whom correspondence should be addressed. Electronic mail: agust@hi.is. Telephone: +354-525-4672 and +354-525-4800. Fax: +354-552-8911.

TABLE I. Observed (2+1) REMPI iodine atomic lines used for laser calibration.

Configuration	Term	J	Ion core	Positions (cm^{-1})[64]
$5s^25p^4(^1D_2)6p$	$^2[1]^\circ$	1/2	$^2P_{1/2}$	72 098.6
$5s^25p^4(^3P_2)5g$	$^2[5]$	11/2 and 9/2	$^2P_{1/2}$	72 285.0
$5s^25p^4(^3P_2)5g$	$^2[4]$	9/2 and 7/2	$^2P_{1/2}$	72 285.1
$5s^25p^4(^1D_2)6p$	$^2[2]^\circ$	3/2	$^2P_{1/2}$	72 436.8
$5s^25p^4(^3P_1)6p$	$^2[2]^\circ$	5/2	$^2P_{3/2}$	72 529.2
$5s^25p^4(^3P_1)6p$	$^2[2]^\circ$	3/2	$^2P_{3/2}$	72 806.4
$5s^25p^4(^3P_2)9p$	$^2[2]^\circ$	3/2	$^2P_{1/2}$	73 013.2
$5s^25p^4(^3P_2)9p$	$^2[2]^\circ$	5/2	$^2P_{1/2}$	73 021.5
$5s^25p^4(^3P_2)9p$	$^2[3]^\circ$	5/2	$^2P_{1/2}$	73 056.1
$5s^25p^4(^3P_2)9p$	$^2[3]^\circ$	7/2	$^2P_{1/2}$	73 058.3
$5s^25p^4(^3P_2)8d$	$^2[1]$	3/2	$^2P_{1/2}$	73 088.0
$5s^25p^4(^3P_2)8d$	$^2[1]$	1/2	$^2P_{1/2}$	73 091.0
$5s^25p^4(^3P_2)9p$	$^2[1]^\circ$	1/2	$^2P_{1/2}$	73 117.9
$5s^25p^4(^3P_1)6p$	$^2[1]^\circ$	1/2	$^2P_{3/2}$	73 387.2

were directed into a time-of-flight tube and detected by a microchannel plate (MCP) detector to record the ion yield as a function of mass and laser radiation wavenumber. Mass signals were recorded by a LeCroy Wavesurfer 44MXs-A, 400 MHz storage oscilloscope. Tunable excitation radiation was generated by an excimer laser-pumped dye laser system, using a Lambda Physik COMPex 205 excimer laser and a Coherent ScanMatePro dye laser, applying a C-540 dye. Laser power was minimized to prevent saturation effects and power broadening. Laser calibration was based on observed (2 + 1) REMPI iodine peaks (see Table I). The accuracy of the calibration was found to be about ±1.0 cm^{-1} on a two-photon wavenumber scale.

III. PERTURBATIONS

For molecular systems, evaluation of the total Hamiltonian can be very onerous. In order to simplify its expression, the Born-Oppenheimer approximation is commonly utilized which involves omitting terms which are the source of observed perturbations in recorded spectra.[56] These are the electronic operator, $\mathbf{H^{el}}$, which is representative of interactions between electronic states, the vibrational operator, $\mathbf{T^N}$, which is representative of interactions between vibrational states, and the spin-orbit operator, $\mathbf{H^{SO}}$, which is representative of interactions between the electron spin and its orbital motion, all of which are homogeneous ($\Delta\Omega = 0$) in nature. The L-uncoupling operator, $(-1/2\mu R^2)(\mathbf{J^+L^-} + \mathbf{J^-L^+})$, and the S-uncoupling operator, $(-1/2\mu R^2)(\mathbf{J^+S^-} + \mathbf{J^-S^+})$, are responsible for heterogeneous ($\Delta\Omega \neq 0$) interactions. The state interaction strength (i.e., the perturbation matrix element, W_{12}, for electronic states, 1 and 2)[57] is independent of the total angular momentum quantum number, J', for homogeneous interactions, but J' dependent for heterogeneous interactions.[56] Such interactions appear as energy level repulsion effects for levels of the interacting states with the same J' values, the degree of which depends on the interaction strength (W_{12}) and the energy mismatch ($\Delta E_{J'}$) of the interacting J' levels,[29,31–33,45,56,58]

$$\Delta E_{J'} = E_{J'}(1) - E_{J'}(2) \tag{1a}$$

for

$$E_{J'}(i) = \frac{1}{2}\left(E^0_{J'}(1) + E^0_{J'}(2)\right) \pm \frac{1}{2}\left[4\,|W_{12}|^2 + \left(E^0_{J'}(1) - E^0_{J'}(2)\right)^2\right]^{1/2}, \quad i = 1,2, \tag{1b}$$

where $E^0_{J'}(1)$ and $E^0_{J'}(2)$ are the zero-order energy levels for the unperturbed states 1 and 2. Furthermore, the interaction involves mixing of the states, fraction of which (c^2(i)) also depends on W_{12} and $\Delta E_{J'}$,[29,31,32,45,56,58] as

$$c^2(i) = \frac{1}{2} \pm \frac{\sqrt{|\Delta E_{J'}|^2 - 4|W_{12}|^2}}{2\,|\Delta E_{J'}|}, \quad \mathrm{i} = 1,2. \tag{2}$$

Repulsion effects and the level of state mixing increase with increasing W_{12} and decreasing $\Delta E_{J'}$. In the limit of $\Delta E_{J'} \approx 0$ where solutions are approximated by "degenerate state perturbation theory"[59,60] which yields very large energy level shifts and state mixings, characteristic for the "near-degenerate" J' levels. Hereby, we shall refer to such cases as "near-degenerate interactions." Furthermore, to distinguish between such cases and cases where interacting levels are non-degenerate[59,60] and perturbations will be less sharply J' dependent, we shall refer to "non-degenerate interactions." We wish to use these expressions to replace the less clear expressions "near-resonance-" and "off-resonance-" interactions, respectively, which have been used before.[29,31–33,39,44–46,58,61]

Interactions between Rydberg and ion-pair states of the hydrogen halides appear distinctively as perturbations in rotationally resolved REMPI spectra, i.e., as deviations in the expected spectral structure of unperturbed states. These deviations can show as line shifts (LS-effects) as a result of the energy level shifts and/or as line-intensity alterations (LI-effects) due to the state mixing which can cause alterations in ion formation paths.[45] Furthermore, perturbations can result in alterations in linewidths on account of different predissociation processes of the mixed states (LW-effect). Observed perturbations, in the spectra of the hydrogen halides, can be classified in the following way:

(a) Weakest effects are found for heterogeneous ($\Delta\Omega \neq 0$), spin forbidden ($\Delta\Sigma \neq 0$) interactions resulting in LI-effects for near-degenerate interactions.[39,44,45,58]
(b) Intermediately strong effects are observed for heterogeneous ($\Delta\Omega \neq 0$), spin conserved ($\Delta\Sigma = 0$) interactions, which typically result in LS-effects for near-degenerate interactions and LI-effects for both near- and non-degenerate interactions.[39,44,45,58]
(c) Strongest effects are seen among homogeneous interactions ($\Delta\Omega = 0$), which show both as LS- and LI- effects both for near-degenerate and non-degenerate interactions.[44,45,58]

Rotational constants for ion-pair vibrational states generally are smaller than those for the interacting Rydberg states. Hence, the energy spacing between J' levels ($\Delta E_{J',J'-1}$) for the Rydberg states is larger than corresponding levels for the ion-pair states.[31–33,44–46,58,61,62] Therefore, near-degenerate interactions, for $\Delta E_{J'} \approx 0$, typically, are observed for one or two J' levels only, whereas non-degenerate interactions can

be observed for a range of J' levels both to higher and lower energies with increasing $|\Delta E_{J'}|$ as J' deviates further away from the near-degenerate levels.[62] Therefore, the non-degenerate interactions show as gradually decreasing LS- and LI-effects, as the J's deviate further away from the near-degenerate J's.

A. LS-effects

To a first approximation, a linear behavior is expected for plots of energy level spacing ($\Delta E_{J',J'-1} = E(J') - E(J'-1)$) vs. J'. Such linearity with a slope of $2B_{v'}$, where $B_{v'}$ is the v′ dependent rotational constant, implies an unperturbed state. Deviations from linearity constitute LS-effects, which are prevalent in (b) and (c) cases mentioned above. The presence of curvatures or irregular shapes in such plots indicates medium to strong state interactions. In order to visualize irregular shapes due to effects of possible near-degenerate interactions more clearly, "reduced term value plots" were also made.[62] These show the difference between observed level energies ($E_{J'}$) and energies, $E^0_{J'}$, given by the expression

$$E^0_{J'} = \nu^0 + B'J'(J'+1) - D'J'^2(J'+1)^2 \qquad (3)$$

for parameters ν^0, B', and D' derived either by deperturbation analysis or by the functional (Eq. (3)) fit to the data points.

B. LI-effects

The REMPI data of the hydrogen halides for resonance excitations to Rydberg or ion-pair states consist of ion signals from both the parent molecule (HX^+) and the atomic fragments (X^+ and H^+). The integrated signals of each respective ion mass reveal relative fractions of the respective formation pathways. The strengths of the ion signals are determined by rates of formation of the resonance excited states, which can involve interference effects as well as the rates of ionization. In the case of a Rydberg to ion-pair state interaction, a relatively large HX^+ signal evidences a large Rydberg state character of the resonance state, whereas a relatively large X^+ signal evidences its large ion-pair state character or an affinity for dissociation. By exploring alterations in the intensity ratio, $I[X^+]/I[HX^+]$ rather than the absolute ion signals ($I[X^+], I[HX^+]$) as a function of J', mixing/interactions of Rydberg and ion-pair states, can be highlighted. Thus, an enhanced intensity ratio, $I[X^+]/I[HX^+]$, with J', for Rydberg resonance states, gives an indication of increased mixing/interactions with an ion-pair state, whereas significant lowering in the ratio would, on the other hand, evidence the opposite, i.e., decreased mixing/interactions with an ion-pair state. It has been found that the overall sensitivity of the LI-effects generally is greater than LS-effects. Thus, for weakly interacting states, there may be a distinctive lack of LS-effects, whereas significant LI-effects may be observed.[31,32,45,61]

C. LW-effects

LW-effects appear as J' dependent alterations in the linewidth of ion signals. To a first approximation, linewidths are inversely proportional to the lifetimes of the resonance excited states and provide a lower limit to their lifetimes. Thus, LW-effects can give indications of lifetimes of rotational levels prior to predissociation. Such predissociation is mainly determined by the rates of crossing from bound to repulsive states. Rydberg states are usually in close proximity to or are crossed by one or more repulsive states whereas the internuclear distance of ion-pair states is too large for curve crossings between ion-pair states and repulsive states to be possible. Therefore, ion-pair states require interactions with Rydberg states, which act as gateway states prior to predissociation.[45,58] Linewidths of ion-pair state spectra are frequently found to be larger (hence lifetimes shorter) than those of Rydberg states, close in energy, suggesting that effective predissociation of ion-pair states can involve several gateway Rydberg states. In REMPI studies of HI,[40,41,44,45] there is a distinct lack of appearances of Rydberg states with $\Omega = 1$. It has been suggested that these states play an important role as gateway states for predissociation processes,[45] acting as dark perturbers or hidden states.

It has been shown that the appearance of LW-effects is intrinsically linked with the appearance of LS- and LI-effects for HBr[58] and HI.[44,45] Thus, the LW-effects are found to show close, but not necessarily equivalent, correspondence to that observed from LS- and LI-effects in terms of J' quantum level dependences.

IV. RESULTS AND ANALYSIS

A. Spectral observations

Figure 1 shows assigned REMPI spectra for HI in the two-photon resonance excitation region of 72 300–74 600 cm^{-1}. A number of new and reassigned Rydberg and ion-pair vibrational states have been detected and analyzed (see details below). The states' characteristics are listed in Tables II and III. $nl\lambda$ type labels are used to characterize the Rydberg electrons, where n is the principal quantum number and the l and λ quantum numbers are replaced by the relevant atomic and molecular orbital letters, respectively. The ion core ($\sigma^2\pi^3$) involves two spin-orbit states, i.e., $\Omega = 1/2, 3/2$.

New Rydberg states were observed with band origins at 72 324.0 cm^{-1} and 73 081.7 cm^{-1} where weak, previously unreported structures, were found in the HI^+ ion spectra (see Figs. 1(a) and 1(b)). These are assigned to the $F^1\Delta_2(v' = 1)$ and $P^1\Delta_2(v' = 0)$ states, respectively. At 72 945.0 cm^{-1} (see Fig. 1(c)), another weak structure was observed in the I^+ spectra. This structure is assigned to the $m^3\Pi_1(v' = 1)$ state. Whereas, it has been detected in absorption,[13] it has not been seen in REMPI before. At 73 384.2 cm^{-1}, a strong, clearly resolved, rotational feature is observed. This feature has previously been reported, unassigned in REMPI,[41] and is here assigned to the $O^1\Sigma^+(v' = 1)$ state (Fig. 1(d)). At 72 923.0 cm^{-1} and 73 110.8 cm^{-1}, new spectral structures were observed mainly in the I^+ and H^+ spectra. Both reveal small rotational constants, $B_{v'}$, and have been assigned to the $V^1\Sigma^+(v' = m + 11)$ and $V^1\Sigma^+(v' = m + 12)$ ion-pair states (see Figs. 1(b) and 1(c)). It should be noted that m denotes an unknown positive integer, since the absolute values of the v′s are uncertain. All other subsequent numberings of previously

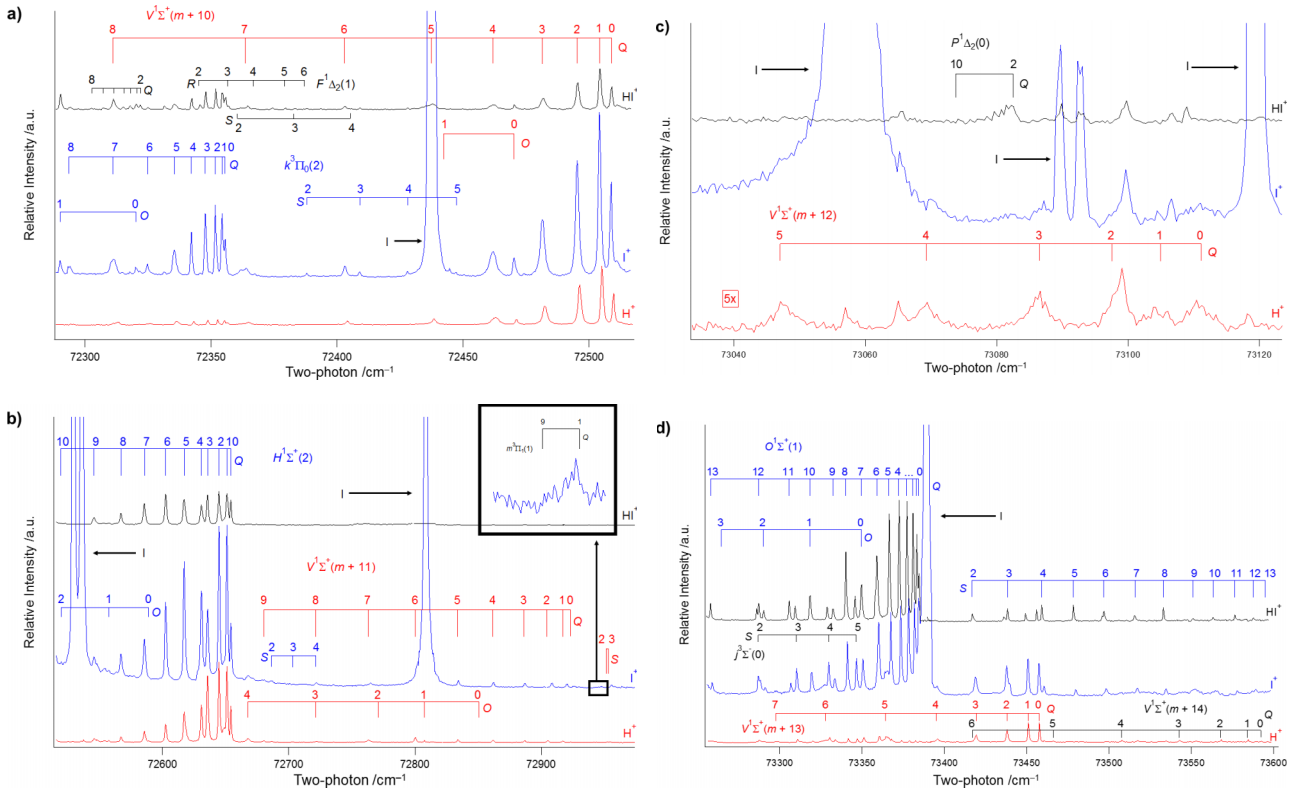

FIG. 1. REMPI spectra for H^+, I^+, and HI^+ and J' assignments of rotational peaks corresponding to two-photon resonance excitation from the ground state to $F^1\Delta_2(v'=1)$ (a), $k^3\Pi_0(v'=2)$ (a), $V^1\Sigma^+(v'=m+10)$ (a); $H^1\Sigma^+(v'=2)$ (b), $V^1\Sigma^+(v'=m+11)$ (b), $m^3\Pi_1(v'=1)$ (b); $P^1\Delta_2(v'=0)$ (c), $V^1\Sigma^+(v'=m+12)$ (c); $j^3\Sigma^-(v'=0)$ (d), $O^1\Sigma^+(v'=1)$ (d), $V^1\Sigma^+(v'=m+13)$ (d), and $V^1\Sigma^+(v'=m+14)$ (d). (2+1) REMPI iodine atomic lines are indicated (see Table I). The H^+ portion of the REMPI spectrum in (c) is magnified (×5).

assigned ion-pair states,[13] upwards from and including the previously assigned $V(m+11)$ ion-pair state, are, therefore, re-assigned as $V(m+i+2)$, where "i" is a positive integer, representing the previous vibrational assignment made by Ginter *et al.*,[13] e.g., $V(m+11)$ is re-assigned as $V(m+13)$ and $V(m+12)$ is re-assigned as $V(m+14)$. Peak positions in the REMPI spectra of all newly observed states are listed in Table IV.

For the subsequent analyses of our observations, the excited states, whose spectra display various types of state interactions, are grouped into four interacting systems. These are the following:

1. The $F^1\Delta_2(v'=1)$, $k^3\Pi_0(v'=2)$, $V^1\Sigma^+(v'=m+10)$ system.
2. The $V^1\Sigma^+(v'=m+10)$, $H^1\Sigma^+(v'=2)$, $V^1\Sigma^+(v'=m+11)$, $m^3\Pi_1(v'=1)$ system.
3. The $P^1\Delta_2(v'=0)$ and $V^1\Sigma^+(v'=m+12)$ states.
4. The $O^1\Sigma^+(v'=1)$, $V^1\Sigma^+(v'=m+13)$, $V^1\Sigma^+(v'=m+14)$, $V^1\Sigma^+(v'=m+15)$ system.

1. The $F^1\Delta_2(v'=1)$, $k^3\Pi_0(v'=2)$, $V^1\Sigma^+(v'=m+10)$ system

Fig. 1(a) shows assigned REMPI spectra for the states of concern. Fig. 2(a) shows the rotational energy levels derived from the spectra. The reasoning behind the assignment of the 72 324.0 cm^{-1} band to the $F^1\Delta_2(1)$ Rydberg state, as mentioned above, is manifold. First, the rotational structure, showing clear Q, R, and S lines for the lowest J' quantum

TABLE II. MO configurations, term symbols, ion core configurations, band origins, rotational parameters, quantum defects, and relative intensities for all Rydberg states observed in the 72 300–74 600 cm^{-1} region.

MO configuration	Term symbols	Ion core	ν^0 (cm^{-1}) This work	ν^0 (cm^{-1}) Others[13]	$B_{v'}$ (cm^{-1}) This work	$B_{v'}$ (cm^{-1}) Others[13]	$D_{v'}$ (cm^{-1}) This work	$D_{v'}$ (cm^{-1}) Others[13]	Quantum defect, δ_l	Intensity
$(\sigma^2\pi^3)6p\pi$	$F^1\Delta_2(1)$	$^2\Pi_{1/2}$	72 324.0	...	6.13	...	0.000 3	...	3.16	w
$(\sigma^2\pi^3)5d\delta$	$k^3\Pi_0(2)$	$^2\Pi_{3/2}$	72 355.6	72 353.1	5.86	5.650	0.004 2	0.000 549	2.35	s
$(\sigma^2\pi^3)5d\pi$	$H^1\Sigma^+(2)$	$^2\Pi_{3/2}$	72 654.3	72 650.8	5.19	5.29	0.000 0	0.000 396	2.32	vs
$(\sigma^2\pi^3)7s\sigma$	$m^3\Pi_1(1)$	$^2\Pi_{3/2}$	72 945.0	72 924.8	6.16	6.205	−0.001 6	0.000 463	4.09	vw
$(\sigma^2\pi^3)4f\pi$	$P^1\Delta_2(0)$	$^2\Pi_{1/2}$	73 081.7	...	6.35	...	0.000 22	...	0.80	vw
$(\sigma^2\pi^3)5d\delta$	$k^3\Pi_1(2)$	$^2\Pi_{3/2}$	73 176.7	73 180.7	6.13	6.034	0.002 3	0.000 872	2.27	m
$(\sigma^2\pi^3)5d\pi$	$j^3\Sigma^-(0)$	$^2\Pi_{1/2}$	73 252.0	73 254.9	5.63	5.706	0.004 6	0.004 75	1.77	vs
$(\sigma^2\pi^3)4f\pi$	$O^1\Sigma^+(1)$	$^2\Pi_{3/2}$	73 384.2	73 383.6	5.70	5.819	0.000	0.000 446	1.04	s

TABLE III. Band origins, rotational parameters, and relative intensities for all ion-pair states observed in the 72 300–74 600 cm^{-1} region.

Ion-pair state, $V(m+i)$	ν^0 (cm^{-1})		$B_{v'}$ (cm^{-1})		$D_{v'}$ (cm^{-1})		
	This work	Others[13]	This work	Others[13]	This work	Others[13]	Intensity
$i=10$	72 508.8	72 506.0	4.25	4.106	0.008 0	0.001 47	s
$i=11$	72 923.0	...	3.43	...	0.001 9	...	m
$i=12$	73 110.8	...	4.34	...	0.001	...	vw
$i=13$	73 459.1	73 457.8	4.52	3.177	0.008 9	−0.002 37	m
$i=14$	73 590.8	73 589.5	2.23	2.294	0.000	−0.001 15	m
$i=15$	73 831.8	73 822.7	4.14	3.769	0.009	−0.000 225	m

level, $J'=2$, is a clear indication of an $\Omega=2$ state. Second, its band origin is 2100.4 cm^{-1} higher than that for the $F^1\Delta_2(0)$ state,[44] which is close to that to expect for an energy difference between $v'=0$ and 1 levels of a pure Rydberg state. For comparison, the energy difference between the $v'=0$ and 1 levels of the ground state ion is 2140 cm^{-1}.[63] Third, spectral analyses give a rotational constant $B_{v'}$ (6.13 cm^{-1}) close to that for the ground state (6.43 cm^{-1})[64] and slightly less than that for the $F^1\Delta_2(0)$ state.[44] Finally, the REMPI spectral structure was mainly found for the HI^+ ions, further supporting the claim of a pure Rydberg state (see Sec. III).

a. LS-effects. Fig. 2(b) shows the spacing between the rotational levels ($\Delta E_{J',J'-1}$) for the $F^1\Delta_2(1)$ and $k^3\Pi_0(2)$ Rydberg states as a function of J' (see also supplementary material in Ref. 62). Whereas no significant deviation from linearity is seen in the plot for the $F^1\Delta_2(1)$ state, a negative curvature is observed for the $k^3\Pi_0(2)$ state. This suggests that the $F^1\Delta_2(1)$ state experiences negligible or very small state interactions, whereas the $k^3\Pi_0(2)$ state undergoes increasing non-degenerate interactions with J'. An inspection of the energy level diagram (Fig. 2(a)) reveals that such an effect is to be expected for an interaction with the $V(m+10)$ state as the spacing between quantum levels with equal J' quantum numbers gradually decreases as J' increases from 0 to 8.

b. LI-effects. The intensity ratio, $I[I^+]/I[HI^+]$, derived from the Q lines for the $k^3\Pi_0(2)$ state, shows a gradual increase with J' from $J'=0$ to 8 with the exception of $J'=7$ (Fig. 2(c)). This indicates that the $k^3\Pi_0(2)$ state experiences increased mixing with the $V(m+10)$ state as J' increases. Furthermore, based on the rotational energy level diagram (see Fig. 2(a)), a near-degenerate interaction between the $k^3\Pi_0(2)$ and the $F^1\Delta_2(1)$ states might be expected for $J'=7$ (and for $J'=8$). Therefore, the drop in the intensity ratio for $J'=7$ is most probably due to mixing of the $k^3\Pi_0(2)$ and $F^1\Delta_2(1)$ states, resulting in changed formation rates of the I^+ and/or HI^+ ions, thus allowing weak near-degenerate interactions, not detectable by line shifts, to be observed. An interaction between the $k^3\Pi_0(2)$ ($\Omega=0$) and the $F^1\Delta_2(1)$ ($\Omega=2$) states, however, requires mixing with an $\Omega=1$ state to fulfill the requirement of $|\Delta\Omega|=1$ state interactions.[56]

c. LW-effects. Fig. 3 shows linewidths of Q rotational lines of spectra for the $k^3\Pi_0(2)$ state (for I^+ ions) and the $V(m+10)$ state (H^+). Similar looking graphs were obtained for other ions (HI^+ for $k^3\Pi_0(2)$, and HI^+ and I^+ for $V(m+10)$). Significant line broadenings are observed for $J'=5$ and $J'=7$–8 in the case of $k^3\Pi_0(2)$, and for $J'\sim4$ and $J'=7$–8 in the case of $V(m+10)$. Generally, the linewidths of the $V(m+10)$ state are larger than the linewidths of the $k^3\Pi_0(2)$ state for $J'=0$–6. They are, however, comparable for $J'=7$–8 within experimental error. These observations can be interpreted in the following way, assuming that variations in the linewidths are determined by a combination of bound state interactions and/or predissociation effects (see above in Sec. III). First, based on the above interpretations of the LS- and LI-effects, the enhanced linewidth for $J'=7(8)$ is most probably associated with the $J'=7$ near-degenerate interaction between the $k^3\Pi_0(2)$ and $F^1\Delta_2(1)$ Rydberg states via a mixed $\Omega=1$ state. Furthermore, as seen from Fig. 2(a),

TABLE IV. Rotational lines for HI due to two-photon resonance transitions to $F^1\Delta_2(v'=1)$, $P^1\Delta_2(v'=0)$, $V^1\Sigma^+(v'=m+12)$, and $V^1\Sigma^+(v'=m+13)$ states.

	$F^1\Delta_2(1)$ (cm^{-1})			$m^3\Pi_1(1)$ (cm^{-1})	$P^1\Delta_2(0)$ (cm^{-1})	$V^1\Sigma^+(m+11)$ (cm^{-1})			$V^1\Sigma^+(m+12)$ (cm^{-1})
J'	Q	R	S	Q	Q	O	Q	S	Q
0						72 850.5	72 923.0		73 110.8
1				72 944.0		72 807.6	72 917.0		73 104.6
2	72 321.7	72 345.3	72 360.4	72 943.2	73 081.1	72 771.2	72 904.5	72 951.3	73 097.2
3	72 320.1	72 356.8	72 382.8	72 942.0	73 080.4	72 721.6	72 886.3	72 952.9	73 086.2
4	72 317.7	72 367.1	72 405.2	72 939.6	73 079.6	72 667.8	72 861.5		73 069.0
5	72 315.0	72 379.3		72 937.6	73 078.6		72 833.7		73 046.7
6	72 311.0	72 387.2		72 936.8	73 077.5		72 800.4		
7	72 306.7			72 935.5	73 076.0		72 762.8		
8	72 302.3			72 934.3	73 074.9		72 721.6		
9					73 073.1		72 680.6		
10							72 644.7		

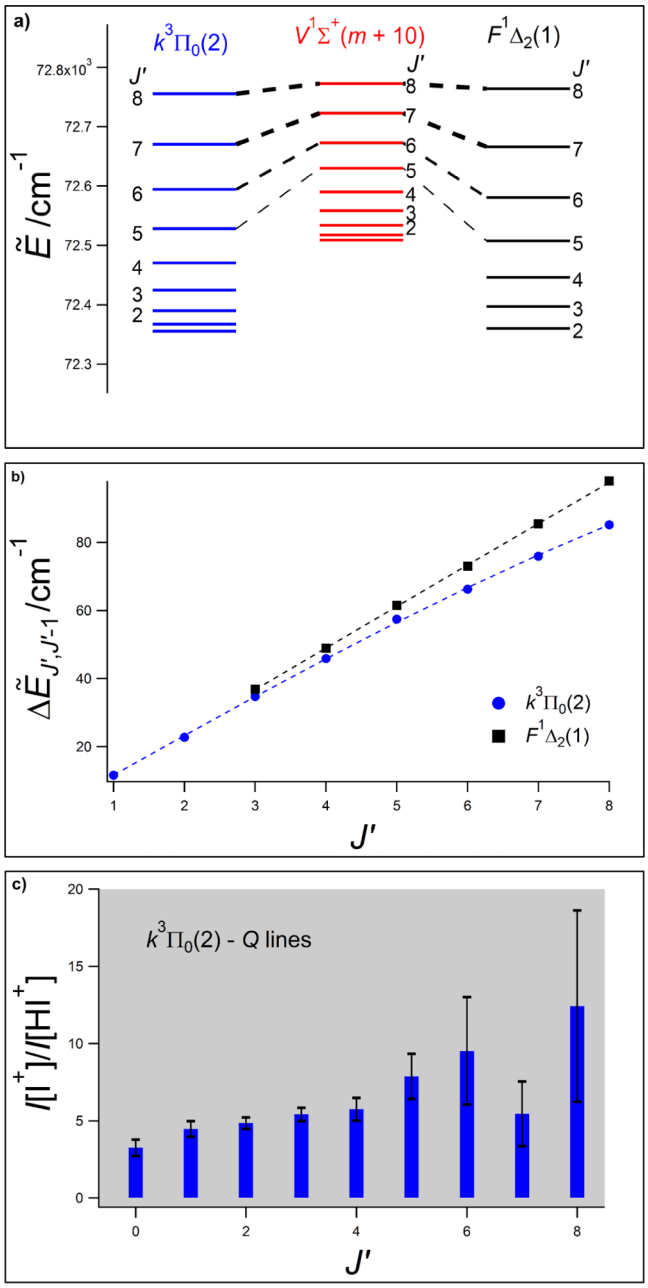

FIG. 2. (a) Rotational energy levels of the $F^1\Delta_2(v'=1)$, $k^3\Pi_0(v'=2)$, and $V^1\Sigma^+(v'=m+10)$ states, derived from the observed REMPI spectra. J' dependent state interactions are also indicated. (b) Spacing between rotational levels ($\Delta E_{J',J'-1}$) as a function of J'; experimental values and fit curves for the $k^3\Pi_0(v'=2)$ and $F^1\Delta_2(v'=1)$ states. (c) Relative ion-signal intensities ($I(I^+)/I(HI^+)$) vs. J' derived from the Q rotational lines for the $k^3\Pi_0(v'=2)$ state.

a relatively large interaction between those states and the $V(m+10)$ state might be expected for $J'=7$–8, since the $J'=8$ levels for all the states (and the $J'=7$ levels to a lesser extent) are near-degenerate. The linewidth increase in $J'=5$ for the $k^3\Pi_0(2)$ state is likely to be associated with near-degenerate interactions. The rotational energy diagram (Fig. 2(a)) signifies, however, that this can neither be due to near-degenerate interactions with the $F^1\Delta_2(1)$ state nor with the $V(m+10)$ state. We, therefore, propose that the $k^3\Pi_0(2)$ state undergoes a near-degenerate interaction, for $J'=5$, with an $\Omega=1$ hidden Rydberg state which plays a pivotal role in the aforementioned interaction between the $k^3\Pi_0(2)$ and $F^1\Delta_2(1)$ states as well as interactions between the $V(m+10)$ ($\Omega=0$) and $F^1\Delta_2(1)$ ($\Omega=2$) states. Thus, the decreased lifetime for $k^3\Pi_0(2)$, $J'=5$ (larger linewidths), will be due to the $\Omega=1$ state's predissociation by one or more of the repulsive valence states, namely, $A^1\Pi_1$, $a^3\Pi_1$, and/or $t^3\Sigma^+$. The $\Omega=1$ state will, then, act as a gateway state towards predissociation of the $k^3\Pi_0(2)$ state. The broader linewidths for $V(m+10)$, $J'\sim4$, could be associated with indirect predissociation of the ion-pair state via interaction with the mixed $k^3\Pi_0(2)$ and $F^1\Delta_2(1)$ states. Finally, large linewidths, hence shorter lifetimes for the $V(m+10)$ levels than for the $k^3\Pi_0(2)$ levels, $J'=0$–6, suggest that interactions of the V state with additional predissociating gateway states are also of importance.

In light of the above observations and interpretations, the hidden Rydberg state characteristics could be guessed. Assuming the $J'=5$ level of the hidden Rydberg state to be close in energy to that of the $J'=5$ level of the $k^3\Pi_0(2)$ state and by using "typical" spectroscopic constants for a HI Rydberg state, its band origin can be estimated to be about $\nu^0\approx72\,400$ cm$^{-1}\pm5$ cm^{-1}. Among singlet or triplet $\Omega=1$ Rydberg states, which could readily interact with the repulsive valence states, higher vibrational levels of any of the previously observed Rydberg states possessing $^1\Pi_1$ or $^3\Pi_1$ symmetry, i.e., $K^1\Pi_1$, $D^1\Pi_1$, $N^1\Pi_1$, $k^3\Pi_1$, $d^3\Pi_1$, and $m^3\Pi_1$ states[44] could be excluded, energetically. We propose that the hidden state, centered near 72 400 cm^{-1} is the $n^3\Pi_1(v'=0)$ ($(\sigma^2\pi^3)5d\sigma$) Rydberg state, which has not been observed before and, furthermore, that the observed perturbation is due to a weak S-uncoupling ($|\Delta\Omega|=1$) interaction.[65]

2. The $V^1\Sigma^+(v'=m+10)$, $H^1\Sigma^+(v'=2)$, $V^1\Sigma^+(v'=m+11)$, $m^3\Pi_1(v'=1)$ system

Fig. 1(b) shows assigned REMPI spectra for the states of concern. Fig. 4(a) shows the rotational energy levels derived from the molecular spectra. The spectrum for the $H^1\Sigma^+(2)$ Rydberg state has been observed before.[13] It should be mentioned that the spectrum was re-assigned in a recent publication.[44] The mass resolved spectra of the Q lines (Fig. 1(b)) all reveal clear perturbations in the form of LS- and/or LI-effects for $J'\sim3$–5. The $m^3\Pi_1(1)$ Rydberg state, previously observed in absorption,[13] is now seen in REMPI for the first time with band origin 72 945.0 cm^{-1}. Only weak Q lines for the I^+ ion are significantly visible. Some weak lines are observed between 72 960 and 73 000 cm^{-1} which could belong to the R and/or S series. These, however, remain unassigned for the time being. With a band origin ν^0 = 72 923.0 cm^{-1} and a rotational constant of $B_{v'}=3.43$ cm^{-1}, a rotational structure was observed mainly for the I^+ and H^+ ions. This system has never been observed before, neither in absorption nor in REMPI. The small rotational constant, the band origin value, the dominating appearance of the structure for the fragment ions, as well as the appearance of O, Q, and S lines, only, make the assignment of the spectrum to the $V(m+11)$ ion-pair state indisputable.

a. LS-effects. Figs. 4(b) and 4(c) show the spacing between the rotational levels for the $H^1\Sigma^+(2)$, $V(m+10)$, and $V(m+11)$ states as a function of J' as well as the correspond-

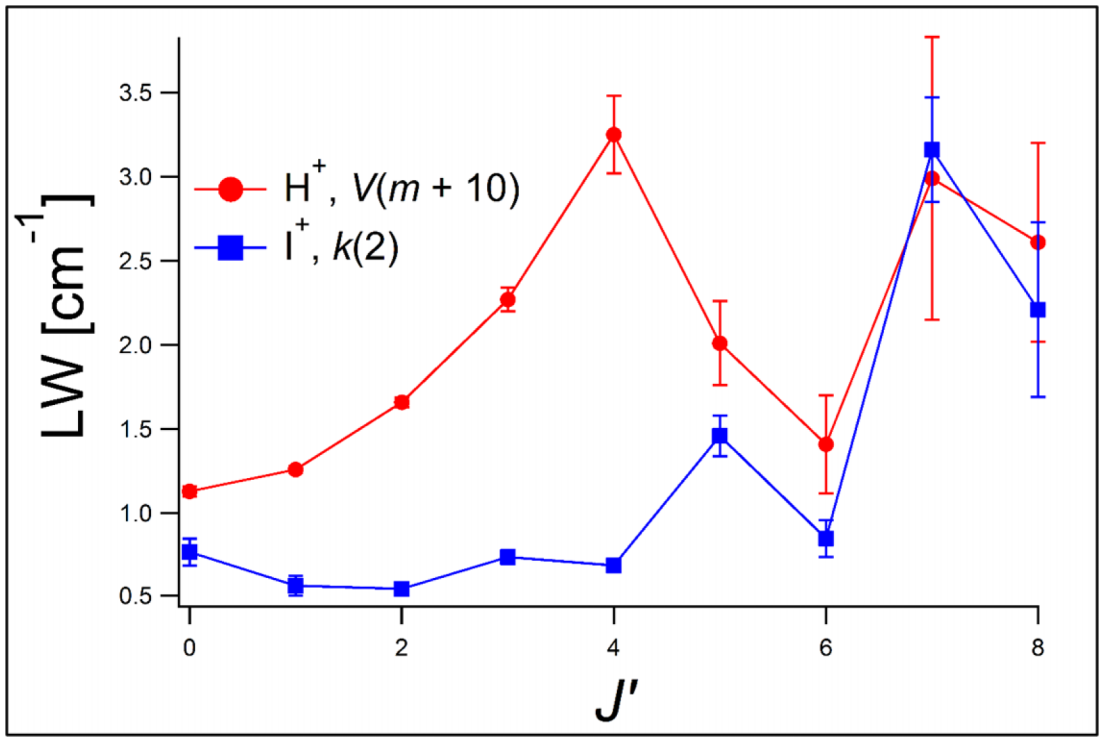

FIG. 3. Rotational linewidths vs. J' derived from the Q lines of the I^+ signal for the $k\,^3\Pi_0(v' = 2)$ state and of the H^+ signals for the $V\,^1\Sigma^+(v' = m + 10)$ state.

ing reduced term value plots. First, irregularities in the plots for $H\,^1\Sigma^+(2)$, appearing as a decrease of the $\Delta E_{3,2}$ and $\Delta E_{5,4}$ values but as an increase of the $\Delta E_{4,3}$ value relative to those of a line fit (unperturbed values), are typical for a near-degenerate interaction. Apart from these irregularities, the $\Delta E_{J',J'-1}$ vs. J' plot for $H\,^1\Sigma^+(2)$ is close to linear. The corresponding plots for the $V(m + 10)$ and $V(m + 11)$ states, on the other hand, show negative and positive curvatures, respectively, suggesting that the ion-pair states experience non-degenerate interactions with the $H\,^1\Sigma^+(2)$ Rydberg state, which is of energy in between and close to those of the $V(m + 10)$ and $V(m + 11)$ states (see Fig. 4(a)). Further inspection of the vibrational energies of the ion-pair vibrational states (see Ref. 44 and Fig. 5) reveals larger energy gap between the $V(m + 10)$ and $V(m + 11)$ states, which is to be expected for vibrational states closest in energy to an interacting $\Omega = 0$ Rydberg state.[44] To verify this and to determine the strength of the interaction between the ion-pair states and the $H\,^1\Sigma^+(2)$ state, a three-state deperturbation analysis was performed, which has been described explicitly in previous publications.[33,45,58] The deperturbation analysis only gave approximate interaction strengths as $W_{H,V(m+11)} = 13 \pm 6$ cm^{-1} and $W_{H,V(m+12)} = 15 \pm 8$ cm^{-1}. The deperturbation results, however, do not explain the interaction effects observed at $J' = 3$–5 in the $H\,^1\Sigma^+(2)$ state nor can they be ascribed to interaction effects of the $m\,^3\Pi_1(1)$ state, which is higher in energy. Therefore, we propose that these effects are caused by interaction with a hidden Rydberg state.

b. LI-effect. Fig. 4(d) shows the intensity ratio, $I[I^+]/I[HI^+]$, derived from the Q lines for the $H\,^1\Sigma^+(2)$ state. Apart from the dip in the ratio for $J' = 3$, it is found to increase with J' from $J' = 0$ to 2 followed by a decrease to $J' = 7$. Comparatively, non-degenerate interactions between $\Omega = 0$ Rydberg states ($E\,^1\Sigma^+$) and ion-pair states, close in energy, for HCl and HBr,[33] display distinctively dissimilar behaviors than analogous interactions between the $H\,^1\Sigma^+$ state and the $V(m + 10)$ and $V(m + 11)$ states. The different trends observed in the intensity ratio for $J' = 0$–7 (Fig. 4(d)) as well as the irregularities in the absolute ion signal intensities (see Fig. 1(b) and text above) must be due to interactions between the $H\,^1\Sigma^+(2)$ state and a hidden Rydberg state. Thus, the state mixing can alter the ionization yield of the otherwise unmixed $H\,^1\Sigma^+(2)$ Rydberg state to increase the I^+ formation and/or decrease the HI^+ formation for $J' \sim 1$, 2 and $J' \sim 4$, 5 and give the ratios shown in Fig. 4(d). This can be due to different ionization rates of the two interacting states.

c. LW-effects. No significant alterations were observed for the rotational linewidths as a function of J' for all the spectra except for the $V(m + 10)$ ion-pair state as mentioned before (see Sec. IV A 1). The average linewidths for the $V(m + 10)$, $V(m + 11)$, $H\,^1\Sigma^+(2)$, and $m\,^3\Pi_1(1)$ states are about 2.1, 1.8, 1.3, and 1.0 cm^{-1}, respectively. Typically, larger linewidths, hence shorter lifetime, are observed for the ion-pair states than for an interacting Rydberg state, again suggesting that interactions of the ion-pair states with more strongly predissociating gateway states are of importance.

Whereas the $m\,^3\Pi_1(1)$ Rydberg state's $\Omega = 2$ counterpart, $m\,^3\Pi_2(1)$, has not been observed in REMPI,[33,36] it has been seen in absorption at about $\nu^0 = 72\,697$ cm^{-1}.[13] Therefore, it could interact with the $H\,^1\Sigma^+(2)$ state ($\nu^0 = 72\,654.3$ cm^{-1}) due to its energetic proximity via mixing with an $\Omega = 1$ state. Furthermore, perturbations have not been observed in the $H\,^1\Sigma^+(2)$ spectra for $J' < 2$,[13] which might suggest that the perturbing state is an $\Omega = 2$ state. Due to the difference

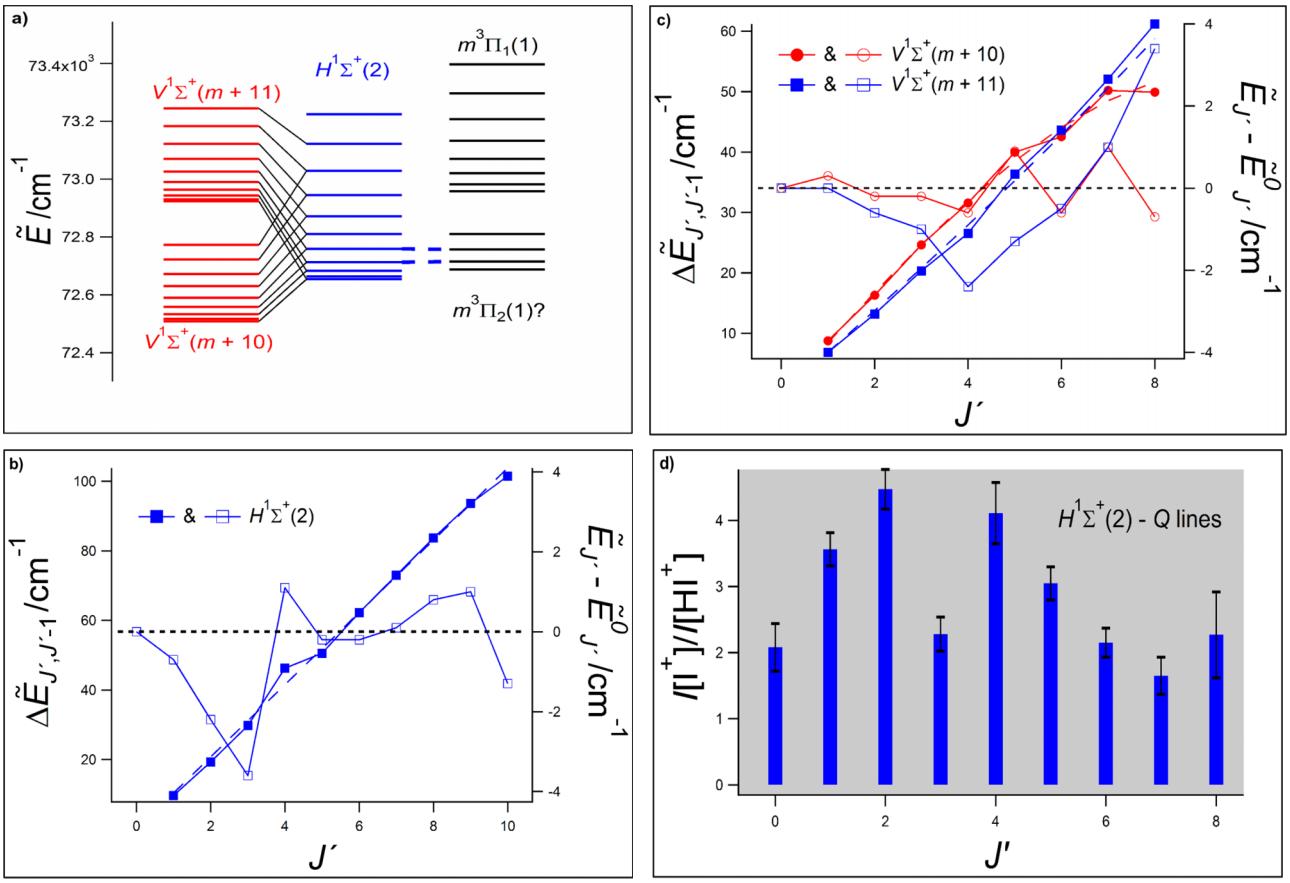

FIG. 4. (a) Rotational energy levels of the $V^1\Sigma^+(v' = m + 10)$, $H^1\Sigma^+(v' = 2)$, $V^1\Sigma^+(v' = m + 11)$ and $m^3\Pi_1(v' = 1)$ states derived from the REMPI spectra as well as rotational energy levels of the $m^3\Pi_2(v' = 1)$ state derived from Ref. 13. Non-degenerate interactions between the $H^1\Sigma^+(v' = 2)$ Rydberg state and the $V^1\Sigma^+(v' = m + 10)$ and $V^1\Sigma^+(v' = m + 11)$ ion-pair states are marked as well as the near-degenerate interactions between the $J' = 3$, 4 rotational levels of the $H^1\Sigma^+(v' = 2)$ Rydberg state and the $m^3\Pi_2(v' = 1)$ state. (b) Spacing between rotational levels ($\Delta E_{J',J'-1}$) as a function of J' (left vertical axis) and the corresponding reduced term value plot (right vertical axis) for the $H^1\Sigma^+(v' = 2)$ state; experimental values (dots joined by lines); and fit curve (dashed blue curve). (c) Spacing between rotational levels ($\Delta E_{J',J'-1}$) as a function of J' (left vertical axis) and the corresponding reduced term value plot (right vertical axis) for the $V^1\Sigma^+(v' = m + 10)$ (red) and $V^1\Sigma^+(v' = m + 11)$ (blue) states; experimental values (dots joined by lines), and fit curve (dotted line). (d) Relative ion-signal intensities ($I(H^+)/I(HI^+)$) vs. J' derived from the Q rotational lines for the $H^1\Sigma^+(v' = 2)$ state.

in the rotational constants for the two states (about 5.19 and 6.16 cm^{-1} for the $H^1\Sigma^+(2)$ and $m^3\Pi_2(1)$ states, respectively), the spacing between the rotational levels of same J' values will increase; hence the mixing will decrease, with J'. On the other hand, the interaction strength (W_{12}) will increase with J' ($W_{12} = W_{12}'(J'(J' + 1))^{1/2}$ for $|\Delta\Omega| = 1$ interactions). Therefore, an increase in interaction strength followed by its decrease as J' increases might be expected, analogous to the behaviour observed for the intensity ratio ($I[I^+]/I[HI^+]$) as a function of J', apart from the dip for $J' = 3$. Therefore, we propose that the hidden state is the $m^3\Pi_2(v' = 1)$ Rydberg state, being hidden in REMPI but observable in absorption.

3. The $P^1\Delta_2(v' = 0)$ and $V^1\Sigma^+(v' = m + 12)$ states

Fig. 1(c) shows assigned REMPI spectra for the states of concern. Fig. 5 shows relevant band origins along with other states, close in energy. The reasoning behind the assignment of the weak band at 73 081.7 cm^{-1} to the $P^1\Delta_2(0)$ Rydberg state, as mentioned above, is manifold. First, the absence of Q rotational lines for $J' < 2$ strongly suggests a state with the total angular momentum of $\Omega = 2$. The rotational constant ($B_{v'} = 6.35$ cm^{-1}) derived from the spectrum is relatively large and comparable to those derived from virtually unperturbed (pure) Rydberg states, such as the $F^1\Delta_2(0)$ ($B_{v'} = 6.32$ cm^{-1}) and $I^1\Delta_2(0)$ ($B_{v'} = 6.31$ cm^{-1}) states.[36,37] An observation of, primarily, the HI^+ signal is also a clear indication of a pure Rydberg state. The state can neither be a vibrationally excited $F^1\Delta_2$ ($(\sigma^2\pi^3)6p\pi$) or $I^1\Delta_2$ ($(\sigma^2\pi^3)5d\pi$) state, since it does not fit into the corresponding vibrational state series. Simple quantum defect analysis,[44,58] based on the expression for vibrational Rydberg state energies ($E_{v'}([\Omega_c, v^+]nl; \omega)$),

$$E_{v'}([\Omega_c, v^+]nl; \omega) = IE([\Omega_c, v^+]) - R/(n^*)^2, \quad (4)$$

was performed. In Eq. (4), v' and v^+ are the vibrational quantum numbers for the Rydberg and ionic states, respectively ($v' = v^+$), and $IE([\Omega_c, v^+])$ is the ionization limit of the molecular ion vibrational state, to which the Rydberg series converges. n^* is the effective principal quantum number depending on the Rydberg electron principal quantum number (n) and the l quantum number dependent quantum defect value (δ_l) as $n^* = n - \delta_l$. The analyses revealed a value

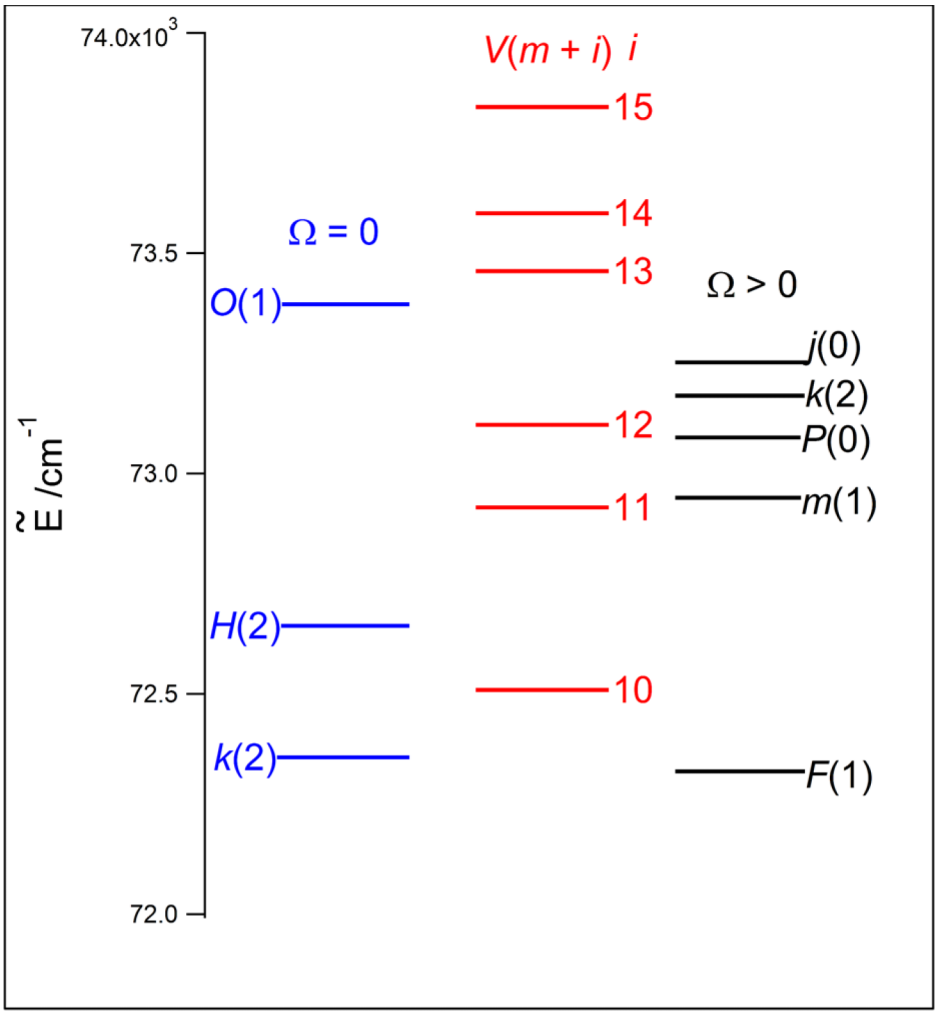

FIG. 5. Energy diagram of the observed electronic states for HI in the two-photon excitation region 72 300–74 600 cm^{-1}. Rydberg states with $\Omega = 0$ total angular momentum are presented in blue to the left, ion-pair states are presented in red (middle) and Rydberg states with $\Omega \neq 0$ total angular momentum are presented in black to the right.

of 0.8 for δ_l, which although quite large, are significantly lower than values derived for d electron Rydberg states (see Table II) and comparable to that previously determined for the $O^1\Sigma^+(v' = 0)$ $((\sigma^2\pi^3)4f\pi)$ state.[44] Therefore, we assign the spectrum centered at 73 081.7 cm^{-1} to the $P^1\Delta_2(v' = 0)$ $((\sigma^2\pi^3)4f\pi)$ Rydberg state. At 73 110.8 cm^{-1}, very weak and broad Q lines are observed for the first time. Analyses gave the rotational constant $B_{v'} = 4.34$ cm^{-1}. The small rotational constant, the band origin value, and a dominating appearance of the structure for the fragment ion H^+ (see Fig. 5) make the assignment of the spectrum to the $V(m + 12)$ ion-pair state indisputable.

a. LS-, LI-, and LW-effects. Although close in energy, there are no indications of interactions between the $P^1\Delta_2(0)$ and $V(m + 12)$ states based on LS- or LI-effects. The linewidths of the Q lines of the $V(m + 12)$ state spectrum are about 3.6 cm^{-1}, on average, whereas the linewidths of the Q lines of the $P^1\Delta_2(0)$ spectrum are close to or just above the detection limit of about 0.3–0.5 cm^{-1}. The linewidths of the $V(m + 12)$ spectrum are found to be larger than those of V-vibrational states closer in energy to neighboring $\Omega = 0$ Rydberg states (see Fig. 5). Thus, the average linewidths of the Q lines for the $V(m + 10)$ and $V(m + 11)$ spectra are about 2.1 and 1.8 cm^{-1}, respectively, and the linewidths of the rotational lines for the lowest J' levels of the $V(m + 13)$ spectrum are less than 1 cm^{-1}. This suggest that interactions of $V(m + 12)$ with the closest in energy $\Omega = 0$ Rydberg states are not the major reason for the broad linewidths observed. More likely, the main reason is a direct heterogeneous interaction with a close in energy $\Omega = 1$ state which acts as a gateway state towards rapid predissociation.

A possible candidate for an $\Omega = 1$ hidden Rydberg state is either of the $M^1\Pi_1$, $(\sigma^2\pi^3)7s\sigma$ or $R^1\Pi_1$, $(\sigma^2\pi^3)7p\sigma$ Rydberg states, both of which have not been observed in absorption or REMPI. Further information, however, are required for a definitive assignment, so for the time being, these proposals are purely conjectured.

4. The $O^1\Sigma^+(v' = 1)$, $V^1\Sigma^+(v' = m + 13)$, $V^1\Sigma^+(v' = m + 14)$, $V^1\Sigma^+(v' = m + 15)$ system

Fig. 1(d) shows assigned REMPI spectra for the states of concern. Fig. 6(a) shows the rotational energy levels derived from the spectra as well as those derived for the $V(m + 15)$ state. The spectrum centered at 73 384.2 cm^{-1} has been assigned before to an $\Omega = 0^+$ Rydberg state.[41] We assign it to the first excited vibrational state of the $O^1\Sigma^+$ state, i.e., the

$O^1\Sigma^+(v' = 1)$ state, since its energy is 2089.5 cm^{-1} higher than that of the $O^1\Sigma^+(v' = 0)$ state, typical for a vibrational energy difference of a Rydberg state.[13,41,44] Furthermore, the quantum defect of the $O^1\Sigma^+(v' = 1)$ state (Table II) equals the quantum defect of the previously reported $O^1\Sigma^+(v' = 0)$ state.[44] The ion-pair state spectra, previously assigned to the $V(m + 11)$, $V(m + 12)$, and $V(m + 13)$ states, now assigned to the $V(m + 13)$, $V(m + 14)$, and $V(m + 15)$ states, respectively (see Secs. IV A 2 and IV A 3), have all been observed in absorption.[13] Perturbation effects, seen in the spectra, have been reported.[13]

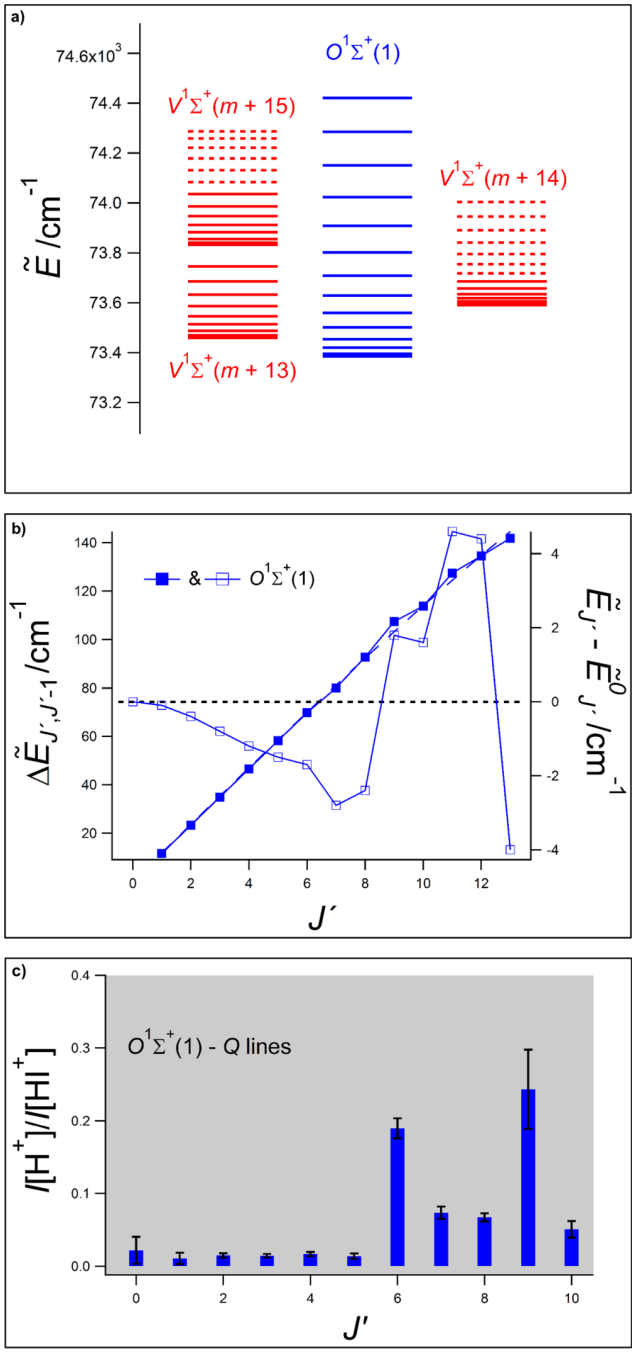

FIG. 6. (a) Rotational energy levels of the $O^1\Sigma^+(v' = 1)$, $V^1\Sigma^+(v' = m + 13)$, $V^1\Sigma^+(v' = m + 14)$, and $V^1\Sigma^+(v' = m + 15)$ states derived from the REMPI spectra. (b) Spacing between rotational levels ($\Delta E_{J',J'-1}$) as a function of J' as well as the corresponding reduced term value plot for the $O^1\Sigma^+(v' = 1)$ Rydberg state; experimental values (dots joined by lines); and fit curve (dotted line). (c) Relative ion-signal intensities ($I(H^+)/I(HI^+)$) vs. J' derived from the Q rotational lines for the $O^1\Sigma^+(v' = 1)$ state.

a. LS- and LI-effects. Fig. 6(b) shows the spacing between the rotational levels ($\Delta E_{J',J'-1}$) for the $O^1\Sigma^+(1)$ Rydberg state as a function of J' as well as the corresponding reduced term value plot. Irregularities in the plots, for $J' \sim 9$, are typical for near-degenerate interactions. Furthermore, there is an indication of interactions for higher $J's$. Intensity ratios, $I(H^+)/I(HI^+)$ as a function of J', derived from the Q lines for the $O^1\Sigma^+(1)$ state also are indicative of a near-degenerate interaction for $J' = 9$ as well as for $J' = 6$ (Fig. 6(c)). Based on the energy levels of the states involved as well as extrapolated values for higher $J's$ (Fig. 6(a)), these observed perturbations are due to near-degenerate interactions with the $V(m + 13)$ and $V(m + 14)$ states for $J' = 6$ and 9, respectively.

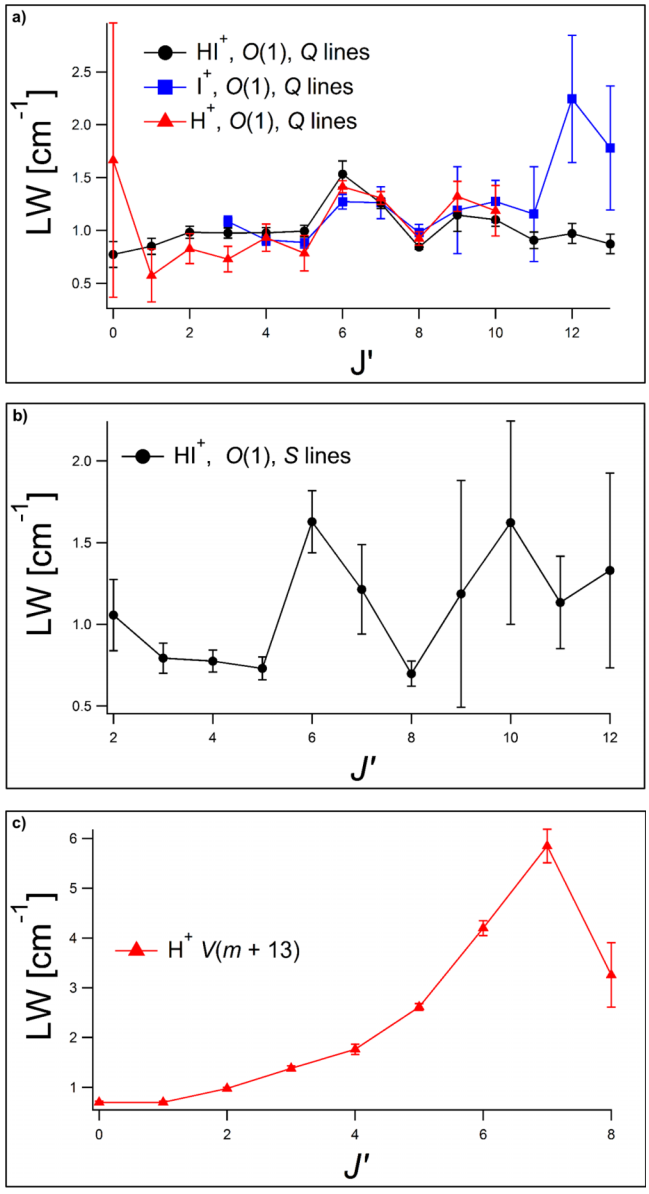

FIG. 7. (a) Rotational linewidths vs. J' derived from the Q lines of the H^+, I^+, and HI^+ signals for the $O^1\Sigma^+(v' = 1)$ state. (b) Rotational linewidths vs. J' derived from the S lines of the HI^+ signals for the $O^1\Sigma^+(v' = 1)$ state. (c) Rotational linewidths vs. J' derived from the Q lines of the H^+ signal for the $V^1\Sigma^+(v' = m + 13)$ ion-pair state.

b. LW-effect. Figs. 7(a)–7(c) show linewidths of rotational lines for the $O^1\Sigma^+(1)$ and $V(m+13)$ spectra. The linewidths for the $O^1\Sigma^+(1)$ state are close to 1 cm^{-1}, on average, whereas those for the $V(m+13)$ state rise with J' from values less than 1 cm^{-1} to about 6 cm^{-1} for $J'=7$. Q and S rotational lines of the $O^1\Sigma^+(1)$ spectrum show line broadening for $J'=6$–7 as well as for $J'=9$–10. Furthermore, the maximum linewidth for $V(m+13)$ is observed for $J'=7$. These observations fit with the LS- and LI-effects seen in the $O^1\Sigma^+(1)$ spectrum (see above), suggesting that it is associated with the coupling between the $O^1\Sigma^+(1)$ state and the $V(m+13)$ and $V(m+14)$ ion-pair states. Considering the larger linewidths of the $J'\sim 5$–8 lines for the $V(m+13)$ state compared with the $O^1\Sigma^+(1)$ state (Figs. 7(a)–7(c)), the lifetime of the coupling states ($J'\sim 6$) must be determined, to some extent, by that of the $V(m+13)$ state which will predissociate via a manifold of gateway Rydberg state(s) (see Sec. III). The rise in the linewidth for the $V(m+13)$ state for $J'\sim 2$–7 is most probably associated with an increasing non-degenerate interaction between the $O^1\Sigma^+(1)$ and $V(m+13)$ states as J' increases.

Whereas the $k^3\Pi_2(v'=0)$ Rydberg state has been observed[13] in this region by absorption at $\nu^0=73\,360.0$ cm^{-1}, it is not seen here. Its lack of appearance might be an indication of the presence of a nearby predissociating $\Omega=1$ hidden Rydberg state, which again could be responsible for the observed "shorter lifetime" of the $V(m+13)$ state.

V. CONCLUSIONS

REMPI spectra of atomic and molecular ions of HI in the two-photon excitation region 72 300–74 600 cm^{-1} were analyzed.

First, the analysis allowed assignments of new spectral structures and characterization of new excited states. New spectral bands at 72 324.0, 73 081.7, 72 923.0, and 73 110.8 cm^{-1} were assigned to the $F^1\Delta_2(1)$ and $P^1\Delta_2(0)$ Rydberg states and the $V^1\Sigma^+(m+11)$ and $V^1\Sigma^+(m+12)$ ion-pair states, respectively. A previously un-assigned spectral structure centered at 73 384.2 cm^{-1} was assigned as the $O^1\Sigma^+(1)$ Rydberg state and the $m^3\Pi_1(1)$ Rydberg state at 72 945.0 cm^{-1} was now observed for the first time in REMPI.

Second, perturbation effects appearing as line shift-, line-intensity-, and linewidth-effects allowed determination of Rydberg to ion-pair as well as Rydberg to Rydberg state interactions both qualitatively and quantitatively. Whereas the line shift and line-intensity effects are primarily indications of bound-to-bound state interactions, the linewidth effects are reflective of direct or indirect (via gateway states) predissociation processes. Generally, it is found that the overall sensitivity of the line-intensity effects is greater than line shift effects. Gradual changes in the various effects as a function of rotational quantum numbers, J', are found to be clear indications of relatively strong homogeneous, non-degenerate interactions between Rydberg and ion-pair states, whereas sudden alterations with J' signals are found to correspond with near-degenerate interactions between Rydberg and ion-pair states or between Rydberg states.

(1) Relatively strong non-degenerate interactions are observed between the states,
   (i) $k^3\Pi_0(v'=2)$ and $V^1\Sigma^+(v'=m+10)$,
   (ii) $H^1\Sigma^+(v'=2)$ and $V^1\Sigma^+(v'=m+10)$,
   (iii) $H^1\Sigma^+(v'=2)$ and $V^1\Sigma^+(v'=m+11)$.
(2) Near-degenerate interactions are observed between the states,
   (i) $k^3\Pi_0(v'=2)$ and $F^1\Delta_2(v'=1)$ ($J'=7$–8),
   (ii) $k^3\Pi_0(v'=2)$ and $V^1\Sigma^+(v'=m+10)$ ($J'=7$–8),
   (iii) $O^1\Sigma^+(v'=1)$ and $V^1\Sigma^+(v'=m+13)$ ($J'=6$),
   (iv) $O^1\Sigma^+(v'=1)$ and $V^1\Sigma^+(v'=m+14)$ ($J'=9$).

Third, the various perturbation effects are found to be indicative of the presence of "hidden states" not observable here, but possibly observable by other technical means. The observed perturbations allowed assignments of these hidden states to some extent.

1. Based on perturbation effects seen in the spectra of the $F^1\Delta_2(1)$, $k^3\Pi_0(2)$ and $V^1\Sigma^+(m+10)$ states, the $n^3\Pi_1(0)$ Rydberg state, centered near 72 400 cm^{-1}, is proposed as a hidden state causing the appearances of LW-effects in the $V^1\Sigma^+(m+10)$ ion-pair state as well as acting as a gateway state to interactions between the $F^1\Delta_2(1)$ Rydberg state and the $k^3\Pi_0(2)$ and $V^1\Sigma^+(m+10)$ states, respectively.
2. The $m^3\Pi_2(1)$ state, centered near 72 697 cm^{-1}, but not observed in REMPI was proposed to be a possible perturber in the $H^1\Sigma^+(2)$ Rydberg state spectrum. Its coupling with the H state would require a mixing with an $\Omega=1$ state, close in energy.
3. Either the $M^1\Pi_1$ or the $R^1\Pi_1$ states are suggested as a possible culprits of rather large linewidths of the $V^1\Sigma^+(m+12)$ ion-pair state.
4. Finally, a hidden $\Omega=1$ Rydberg state, causing the $k^3\Pi_2(0)$ state to be unseen in REMPI due to predissociation, is proposed.

In all the cases (1–4), above, $\Omega=1$ states are believed to be involved, directly or indirectly, as hidden states. This harmonizes with previous findings for the hydrogen halides.[27,29,31–33,45,58] A likely reason for the elusiveness of interacting $\Omega=1$ states is their short lifetimes due to predissociation, but out of six repulsive valence states, which converge to $H(n=1)+I(^2P_{3/2,1/2})$, three are $\Omega=1$ states.

ACKNOWLEDGMENTS

The financial support of the University Research Fund, University of Iceland, and the Icelandic Science Foundation (Grant No. 130259-051) is gratefully acknowledged.

[1]M. J. Simpson, R. P. Tuckett, K. F. Dunn, C. A. Hunniford, and C. J. Latimer, J. Chem. Phys. **130**, 194302 (2009).
[2]J. H. Seinfeld and S. N. Pandis, *Atmospheric Chemistry and Physics: From Air Pollution to Climate Change* (John Wiley & Sons, 2006).
[3]J. I. Lunine, *Astrobiology* (Pearson Addison Wesley, 2005).
[4]A. M. Shaw, *Astrochemistry: From Astronomy to Astrobiology* (Wiley, 2006).
[5]N. Hoffmann, Chem. Rev. **108**, 1052 (2008).
[6]J. B. Nee, M. Suto, and L. C. Lee, J. Chem. Phys. **85**, 719 (1986).
[7]D. S. Ginter and M. L. Ginter, J. Mol. Spectrosc. **90**, 177 (1981).

[8]S. G. Tilford, M. L. Ginter, and J. T. Vanderslice, J. Mol. Spectrosc. **33**, 505 (1970).
[9]J. B. Nee, M. Suto, and L. C. Lee, J. Chem. Phys. **85**, 4919 (1986).
[10]D. S. Ginter, M. L. Ginter, and S. G. Tilford, J. Mol. Spectrosc. **90**, 152 (1981).
[11]R. F. Barrow and J. G. Stamper, Proc. R. Soc. A **263**, 277 (1961).
[12]R. F. Barrow and J. G. Stamper, Proc. R. Soc. A **263**, 259 (1961).
[13]D. S. Ginter, M. L. Ginter, and S. G. Tilford, J. Mol. Spectrosc. **92**, 40 (1982).
[14]M. L. Ginter, S. G. Tilford, and A. M. Bass, J. Mol. Spectrosc. **57**, 271 (1975).
[15]S. G. Tilford, M. L. Ginter, and A. M. Bass, J. Mol. Spectrosc. **34**, 327 (1970).
[16]T. A. Spiglanin, D. W. Chandler, and D. H. Parker, Chem. Phys. Lett. **137**, 414 (1987).
[17]E. de Beer, B. G. Koenders, M. P. Koopmans, and C. A. de Lange, J. Chem. Soc., Faraday Trans. **86**, 2035 (1990).
[18]K. Wang and V. McKoy, J. Chem. Phys. **95**, 8718 (1991).
[19]Y. Xie, P. T. A. Reilly, S. Chilukuri, and R. J. Gordon, J. Chem. Phys. **95**, 854 (1991).
[20]D. S. Green, G. A. Bickel, and S. C. Wallace, J. Mol. Spectrosc. **150**, 303 (1991).
[21]D. S. Green, G. A. Bickel, and S. C. Wallace, J. Mol. Spectrosc. **150**, 354 (1991).
[22]D. S. Green, G. A. Bickel, and S. C. Wallace, J. Mol. Spectrosc. **150**, 388 (1991).
[23]D. S. Green and S. C. Wallace, J. Chem. Phys. **96**, 5857 (1992).
[24]E. de Beer, W. J. Buma, and C. A. deLange, J. Chem. Phys. **99**, 3252 (1993).
[25]P. M. Regan, S. R. Langford, D. Ascenzi, P. A. Cook, A. J. Orr-Ewing, and M. N. R. Ashfold, Phys. Chem. Chem. Phys. **1**, 3247 (1999).
[26]Á. Kvaran, H. Wang, and Á. Logadóttir, J. Chem. Phys. **112**, 10811 (2000).
[27]Á. Kvaran, H. Wang, and B. G. Waage, Can. J. Phys. **79**, 197 (2001).
[28]H. Wang and Á. Kvaran, J. Mol. Struct. **563**, 235 (2001).
[29]Á. Kvaran, H. S. Wang, K. Matthiasson, A. Bodi, and E. Jonsson, J. Chem. Phys. **129**, 164313 (2008).
[30]K. Matthiasson, H. S. Wang, and Á. Kvaran, J. Mol. Spectrosc. **255**, 1 (2009).
[31]Á. Kvaran, K. Matthiasson, and H. S. Wang, J. Chem. Phys. **131**, 044324 (2009).
[32]K. Matthiasson, J. M. Long, H. S. Wang, and Á. Kvaran, J. Chem. Phys. **134**, 164302 (2011).
[33]J. Long, H. Wang, and Á. Kvaran, J. Chem. Phys. **138**, 044308 (2013).
[34]R. Callaghan and R. J. Gordon, J. Chem. Phys. **93**, 4624 (1990).
[35]K. Wang and V. McKoy, J. Chem. Phys. **95**, 7872 (1991).
[36]A. E. Belikov, M. M. Ahern, and M. A. Smith, Chem. Phys. **234**, 195 (1998).
[37]Á. Kvaran, B. G. Waage, and H. Wang, J. Chem. Phys. **113**, 1755 (2000).
[38]D. Ascenzi, S. Langford, M. Ashfold, and A. Orr-Ewing, Phys. Chem. Chem. Phys. **3**, 29 (2001).
[39]J. Long, H. Wang, and Á. Kvaran, J. Mol. Spectrosc. **282**, 20 (2012).
[40]S. A. Wright and J. D. McDonald, J. Chem. Phys. **101**, 238 (1994).
[41]S. T. Pratt and M. L. Ginter, J. Chem. Phys. **102**, 1882 (1995).
[42]Á. Kvaran, Á. Logadóttir, and H. Wang, J. Chem. Phys. **109**, 5856 (1998).
[43]P. M. Regan, D. Ascenzi, E. Wrede, P. A. Cook, M. N. R. Ashfold, and A. J. Orr-Ewing, Phys. Chem. Chem. Phys. **2**, 5364 (2000).
[44]H. R. Hróðmarsson, H. S. Wang, and Á. Kvaran, J. Mol. Spectrosc. **290**, 5 (2013).
[45]H. R. Hróðmarsson, H. S. Wang, and Á. Kvaran, J. Chem. Phys. **140**, 244304 (2014).
[46]D. Zaouris, A. Kartakoullis, P. Glodic, P. C. Samartzis, H. R. Hróðmarsson, and Á. Kvaran, Phys. Chem. Chem. Phys. **17**, 10468 (2015).
[47]S. Kauczok, C. Maul, A. I. Chichinin, and K. H. Gericke, J. Chem. Phys. **133**, 024301 (2010).
[48]C. Romanescu and H. P. Loock, J. Chem. Phys. **127**, 124304 (2007).
[49]C. Romanescu and H. P. Loock, Phys. Chem. Chem. Phys. **8**, 2940 (2006).
[50]C. Romanescu, S. Manzhos, D. Boldovsky, J. Clarke, and H. Loock, J. Chem. Phys. **120**, 767 (2004).
[51]H. P. Loock, C. Romanescu, and S. Manzhos, Abstr. Pap. Am. Chem. Soc. **223**, C19 (2002).
[52]H. P. Loock, B. L. G. Bakker, and D. H. Parker, Can. J. Phys. **79**, 211 (2001).
[53]J. Brown and A. Carrington, *Rotational Spectroscopy of Diatomic Molecules* (Cambridge University Press, Cambridge, United Kingdom, 2003).
[54]W. C. Price, Proc. R. Soc. A **167**, 216 (1938).
[55]D. S. Ginter, M. L. Ginter, S. G. Tilford, and A. M. Bass, J. Mol. Spectrosc. **92**, 55 (1982).
[56]H. Lefebvre-Brion and R. W. Field, *Perturbations in the Spectra of Diatomic Molecules* (Academic Press, Inc., London, 1986).
[57]G. Herzberg, *Molecular Spectra and Molecular Structure: I. Spectra of Diatomic Molecules, Molecular Spectra and Molecular Structure*, 2nd ed. (Van Nostrand Reinhold Company, New York, 1950).
[58]J. Long, H. R. Hróðmarsson, H. Wang, and Á. Kvaran, J. Chem. Phys. **136**, 214315 (2012).
[59]P. A. M. Dirac, *The Principles of Quantum Mechanics* (Oxford University Press, 1930).
[60]D. Bohm, *Quantum Theory* (Dover Publications, New York, 1951).
[61]J. Long, H. Wang, and Á. Kvaran, Acta Phys. Sin. **62**, 163302 (2013).
[62]See supplementary material at http://dx.doi.org/10.1063/1.4922892 for LS- and reduced term value plots and further distinction between near- and non-degenerate perturbations.
[63]N. Böwering, H. W. Klausing, M. Muller, M. Salzmann, and U. Heinzmann, Chem. Phys. Lett. **189**, 467 (1992).
[64]See http://webbook.nist.gov/chemistry/for-ser.html.en-us.en for NIST, 2015.
[65]M. H. Alexander, X. N. Li, R. Liyanage, and R. J. Gordon, Chem. Phys. **231**, 331 (1998).